Supercontinuum generation in hydrogenated amorphous silicon waveguides at telecommunication wavelengths

Jassem Safioui,[1,*] François Leo,[2] Bart Kuyken,[2] Shankar Kumar Selvaraja,[2] Roel Baets,[2] Philippe Emplit,[1] Gunther Roelkens,[2] and Serge Massar[3]

[1]Service OPERA-Photonique, Université Libre de Bruxelles (ULB), 50 Avenue F. D. Roosevelt, CP 194/5, B-1050 Bruxelles, Belgium

[2]Photonics Research Group, INTEC Department, Ghent University-IMEC, Sint-Pietersnieuwstraat 41, 9000 Ghent, Belgium

[3]Laboratoire d'Information Quantique (LIQ), Université Libre de Bruxelles (ULB), 50 Avenue F. D. Roosevelt, CP 225, B-1050 Bruxelles, Belgium

[*]jsafioui@ulb.ac.be

Abstract: We report supercontinuum (SC) generation centered on the telecommunication C-band (1550 nm) in CMOS compatible hydrogenated amorphous silicon waveguides. A broadening of more than 550nm is obtained in 1cm long waveguides of different widths using as pump picosecond pulses with on chip peak power as low as 4W.

OCIS codes: (130.4310) Nonlinear; (320.6629) Supercontinuum generation.

References and links

1. R. R. Alfano, *The Supercontinuum Laser Source*, (2d ed., Springer, New York, 2006).
2. J. M. Dudley, G. Genty and S. Coen, "Supercontinuum generation in photonic crystal fiber," Rev. Mod. Phys **78**, 1135-1184 (2006).
3. E. A. De Souza, M. C. Nuss, W. H. Knox, and D. A. B. Miller, "Wavelength-division multiplexing with femtosecond pulses," Opt. Lett. **20**, 1166-1168 (1995).
4. Th. Udem, R. Holzwarth, T.W. Hänsch, "Optical frequency metrology" Nature **416**, 233-237 (2002).
5. Hideaki Kano and Hiro-o Hamaguchi, "Vibrationally resonant imaging of a single living cell by supercontinuum-based multiplex coherent anti-Stokes Raman scattering microspectroscopy," Opt. Express **13**, 1322-1327 (2005).
6. M. R. E. Lamont, B. Luther-Davies, D. Y. Choi, S. Madden, and B. J. Eggleton, "Supercontinuum generation in dispersion engineered highly nonlinear (γ =10 /W/m) As2S3) chalcogenide planar waveguide," Opt. Express **16**, 14938–14944 (2008).
7. D. Duchesne, M. Peccianti, M. R. E. Lamont, M. Ferrera, L. Razzari, F. Légaré, R. Morandotti, S. Chu, B. E. Little, and D. J. Moss, "Supercontinuum generation in a high index doped silica glass spiral waveguide, " Opt. Express **18**, 923-930 (2010).
8. R. Halir, Y. Okawachi, J. S. Levy, M. A. Foster, M. Lipson, and A. L. Gaeta, "Ultra broadband supercontinuum generation in a CMOS-compatible platform," Opt. Lett **37**, 1685-1687 (2012).
9. L. Yin, Q. Lin, and G. P. Agrawal, "Soliton fission and supercontinuum generation in silicon waveguides," Opt. Lett **32**, 391-393 (2007).
10. I. W. Hsieh, X. Chen, X. Liu, J. I. Dadap, N. C. Panoiu, C. Y. Chou, F. Xia, W. M. Green, Y. A. Vlasov, and R. M. Osgood, "Supercontinuum generation in silicon photonic wires," Opt. Express **15**, 15242-15249 (2007).
11. A. Demircan and U. Bandelow, "Analysis of the interplay between soliton fission and modulation instability in supercontinuum generation," Appl. Phys. B **86**, 31-39 (2007).
12. A. Baldeck, P. L., and R. R. Alfano, "Intensity effects on the stimulated four photon spectra generated by picosecond pulses in optical fibers," J. Lightwave Technol **LT-5**, 1712–1715 (1987).
13. B. Kuyken, X. Liu, R. M. Osgood, Jr., R. Baets, G. Roelkens, and W. M. J. Green, "Mid-infrared to telecom-band supercontinuum generation in highly nonlinear silicon-on-insulator wire waveguides," Opt. Express **19**, 172–181 (2011).
14. Y. Shoji, T. Ogasawara, T. Kamei, Y. Sakakibara, S. Suda, K. Kintaka, H. Kawashima, M. Okano, T. Hasama, H. Ishikawa, and M. Mori, "Ultrafast nonlinear effects in hydrogenated amorphous silicon wire waveguide," Opt. Express **18**, 5668–5673 (2010).

15. K. Narayanan and S. F. Preble, "Optical nonlinearities in hydrogenated-amorphous silicon waveguides," Opt. Express **18**, 8998–9005 (2010).
16. J. Matres, G. C. Ballesteros, P. Gautier, J-M Fédéli, J. Martí, and C. J. Oton, "High nonlinear figure-of-merit amorphous silicon waveguides," Opt. Express **21**, 3932-3940 (2013).
17. C. Grillet, L. Carletti, C. Monat, P. Grosse, B. Ben Bakir, S. Menezo, J. M. Fedeli, and D. J. Moss, "Amorphous silicon nanowires combining high nonlinearity, FOM and optical stability," Opt. Express **20**, 22609-22615 (2012).
18. B. Kuyken, S. Clemmen, S. K. Selvaraja, W. Bogaerts, D. V. Thourhout, P. Emplit, S. Massar, G. Roelkens, and R. Baets, "On-chip parametric amplification with 26.5dB gain at telecommunication wavelengths using CMOS-compatible hydrogenated amorphous silicon waveguides," Optics letters **36,** 552-554 (2011).
19. W. Ke-Yao and A. C. Foster. "Ultralow power continuous-wave frequency conversion in hydrogenated amorphous silicon waveguides." Optics letters **37**, 1331-1333 (2012)
20. S. Uvin, U.D. Dave, B. Kuyken, S. Selvaraja, F. Leo, G. Roelkens, Mid-infrared to telecom-band stable supercontinuum generation in hydrogenated amorphous silicon waveguides, IEEE Photonics Conference 2013 (IPC), United States, p. paper WB2.3 (2013).
21. B. Kuyken, H. Ji, S. Clemmen, S. K. Selvaraja, H. Hu, M. Pu, M. Galili, P. Jeppesen, G. Morthier, S. Massar, L.K. Oxenløwe, G. Roelkens, and R. Baets, "Nonlinear properties of and nonlinear processing in hydrogenated amorphous silicon waveguides," Optics express **19**, B146-B153 (2011).
22. A. Hasegawa and W. F. Brinkman, "Tunable Coherent IR and FIR Sources Utilizing Modulational Instability," IEEE J. Quantum Electron **16**, 694-697 (1980).
23. T. Deschaines, J. Hodkiewicz, P. Henson, "Characterization of Amorphous and Microcrystalline Silicon using Raman Spectroscopy" Thermo Fisher Scientific, Madison, WI, USA.
24. N. Akhmediev and M. Karlsson, "Cherenkov radiation emitted by solitons in optical fibers," Phys. Rev. A **51** 2602–2607 (1995).
25. A. Mussot, E. Lantz, H. Maillotte, T. Sylvestre, C. Finot, and S. Pitois, "Spectral broadening of a partially coherent CW laser beam in single-mode optical fibers," Opt. Express **12**, 2838–2843 (2004).
26. J. M. Dudley, G. Genty, F. Dias, B. Kibler, and N. Akhmediev, "Modulation instability, Akhmediev Breathers and continuous wave supercontinuum generation," Opt. Express **17**, 21497–21508 (2009).
27. D. L. Staebler and C. R. Wronski, "Reversible conductivity changes in discharge-produced amorphous Si," Appl.Phys. Lett **31**, 292–294 (1977).
28. M. Stutzmann, W. B. Jackson, and C. C. Tsai, "Kinetics of the Staebler–Wronski effect in hydrogenated amorphous silicon," Appl. Phys. Lett 45, 1075–1077 (1984).
29. G. P. Agrawal, *Nonlinear fiber optics,* (Optics and Photonics, 3rd ed., Ac. Press, San Diego, 2001).

1. Introduction

Supercontinuum (SC) generation is a large spectral broadening that arises during propagation of a light pulse in a transparent nonlinear material. With appropriate dispersion of the nonlinear medium, strongly broadened spectra have been observed in a variety of media (solids, liquids and gases) [1]. However, the very high pump power required to observe supercontinuum generation in these bulk devices limits their application potential. With the advent of microstructured fibers [2], which allow increasing the effective nonlinearity and provide control over the group velocity dispersion, bright supercontinuum sources can be obtained with low pump pulse energies. This transformed SC generation into a mature field, with several commercial applications such as wavelength division multiplexing (WDM) communication [3], optical frequency metrology [4] and biophotonics [5].

Today, the integration of SC sources is a hot topic, with promising results obtained in compact devices [6-8]. On-chip SC generation has the potential of providing integrated components with small footprints that can be fabricated at low cost and in high volumes. Silicon-on-insulator (SOI) waveguides, thanks to their CMOS compatibility and high nonlinearity, are one of the most promising ultra-compact nonlinear devices for SC generation. In 2007 Yin et al. [9] reported the first numerical simulations of SC generation in a 1.2 cm long crystalline silicon waveguide extending over 400 nm, when a 50 fs pulse at 1.55 μm propagates as a third-order soliton. Promptly after, Hsieh et al. published the experimental demonstration in a 4.7 mm long crystalline silicon waveguide [10], using a 100 fs pulse. A spectral broadening of

approximately 300 nm was obtained at 1.55 μm. In both cases two photons absorption (TPA) clamps the maximum power in the chip, thereby limiting the maximum achievable spectral broadening.

In both studies, the waveguides were engineered to exhibit anomalous group velocity dispersion. Contrary to the normal dispersion regime where due to poor phase-matching the main nonlinear process is self phase modulation (SPM) [11, 12], the anomalous dispersion regime allows in addition to SPM many other nonlinear effects such as, modulation instability, soliton shift, soliton fission and Cherenkov radiation [2]. The combination of some or all these effects allows maximum spectral broadening of the SC. In crystalline silicon nanowires using femtosecond pulses, SPM and soliton fission were the main nonlinear processes reported in [9, 10].

Using picosecond pulsed pump lasers represents another interesting regime in which cascaded four-wave mixing (FWM), modulation instability (MI), SPM and Raman scattering are the most important nonlinear processes involved in SC generation in anomalous dispersion waveguides. Recently, the combination of all these effects was reported to be responsible for the demonstration of SC generation in a 2 cm crystalline silicon waveguide spanning three-quarters of an octave from 1535 to 2525 nm [13]. This broad bandwidth was achieved by using a 2.14 μm wavelength picosecond pump laser. At this pump photon energy, which lies close to the half-bandgap energy of crystalline silicon, the effects of TPA and free carriers absorption are strongly reduced, thereby allowing stronger nonlinear effects.

Recently, attention has focused on using hydrogenated amorphous silicon (a-Si-H) waveguides [14-21]. This material is characterized by a larger band-gap than crystalline silicon, resulting in a lower TPA absorption and a significantly higher figure of merit ($FOM = \gamma_{real} / 4\pi\gamma_{im}$, where γ_{real} and γ_{im} are the real and the imaginary parts of the nonlinear parameter γ , respectively.) at telecom wavelengths [16, 17]. Several nonlinear functions such as parametric amplification [18], frequency conversion [19] and all-optical signal processing [21] were demonstrated.

The major drawback of this material at telecommunication wavelength is optical degradation which has been reported in some experiments when injecting high pump power into the waveguides [21]. We have measured that the optical degradation can be attributed to an increase of the linear and nonlinear losses, resulting in a decrease over time of the nonlinear efficiency. (More information on optical degradation will be provided in a forthcoming paper). However a-Si-H waveguides that do not exhibit optical degradation have also been reported, when short pump pulses are used (1ps <FWHM< 1.8ps) [16, 17].

In this work, we demonstrate, by exploiting its high FOM, SC generation in a-Si-H waveguides at telecommunication wavelengths using picosecond pulses. We investigate the SC in waveguides of different widths ranging from 500 nm to 800 nm (nominally 220 nm thickness), which changes the dispersion of the waveguide. Correspondingly we observe large changes in the bandwidth of the SC. In the wider waveguides that produce the broadest SC, the output spectra show good stability even after several hours of continuous exposure to the high peak power pulse train.

2. Experiment and results

The a-Si-H waveguides are fabricated in a 220 nm-thick hydrogenated amorphous silicon layer deposited on top of a silicon dioxide layer using a low temperature Plasma Enhanced Chemical Vapor Deposition (PECVD) process. The a-Si-H film was formed by plasma decomposition of silane (SiH_4) gas combined with Helium (He) for dilution. Waveguides of varying lengths L (1 to 7cm) and cross section (500×220 nm^2, 700×220 nm^2, 750×220 nm^2 and 800×220 nm^2) were fabricated using 193 nm optical lithography and dry etching.

As a first step, at low power, we estimated the propagation losses for TE polarization of waveguides of different width, see Table 1.

Table 1. Linear and nonlinear losses as a function of waveguides width

Waveguides Width (nm)	500	700	750	800
Linear losses α (dB/cm)	-2.4	-2±1	-2±1	-2±1
Nonlinear losses γ_{im} $W^{-1}m^{-1}$	31	19±3	19±2.5	18±4

Then, to obtain the nonlinear absorption for each waveguide we measured the transmission T as a function of peak power using 1.6ps pulses generated by a picosecond laser source. Using the equation:

$$\frac{1}{T} = \exp(\alpha L) L_{eff} 2\gamma_{im} P + \exp(\alpha L) \tag{1}$$

where, $L_{eff} = (1 - \exp(-\alpha L))/\alpha$ and P are the effective length and optical input power respectively, the nonlinear losses coefficient γ_{im}, originating essentially from TPA, is determined for L=1 cm long waveguides of different width, as shown in Table 1. The broader waveguides have lower non linear losses, which can be attributed to the lower power density in these waveguides.

The high index contrast between silicon and the surrounding media (air or SiO_2), which gives rise to strong optical confinement, results in a high effective nonlinearity parameter γ_{real} of the a-Si-H waveguides. Consequently, and due to the comparatively low nonlinear absorption, the nonlinear FOM ($FOM = \gamma_{real}/4\pi \times \gamma_{im}$) was found to be greater than 2 at telecommunication wavelengths [16-18], thereby paving the way to efficient nonlinear photonic applications.

The high optical confinement contributes also to a waveguide geometry induced anomalous dispersion at telecommunication wavelengths. This anomalous dispersion provides the phase matching conditions necessary for the appearance of the nonlinear effects responsible for the SC generation.

For the experimental demonstration of SC generation, a telecommunication wavelength picosecond pulse train (0.8 ps < FWHM < 1.6 ps depending on the center wavelength, and with a repetition rate of 10 MHz) generated by a tunable optical fiber cavity is used as the pump. In a first experiment, we used the waveguide with a 500×220 nm^2 cross section and 1 cm length. In waveguides with similar cross section, SPM and MI in the picosecond regime were already reported [18, 21]. The coupling between the lensed fibers and the tapered waveguide are estimated to be 6-7 dB. The output beam is sent into a mid-IR optical spectrum analyzer (OSA) at a 1 nm resolution for analysis.

Figure 1 shows the dependence of the output spectrum as a function of on chip peak pump power at a pump center wavelength of λ_{pump}=1560 nm (FWHM≈1 ps). At low pump power, the spectral width varies only slightly. However, above a threshold pump power many peaks appear and the spectral width increases sharply until at the highest on chip peak power of 15.1W, the spectral width has increased to reach a value more than 300 nm at -30 dB from the pump peak.

To determine the nonlinear processes involved in this widening, we investigate the evolution

of the spectrum as a function of the power.
Even at the lowest input power, the pump spectrum is broadened by SPM. When the on chip pump peak power reaches 2.4W the spectrum is further broadened by SPM and two MI sidebands due to the amplification of background noise at wavelengths for which the phase matching condition is satisfied, detuned by approximately 24nm from the pump wavelength, as shown in Fig. 1. Peaks due to higher order sidebands that are created when the first order sidebands become strong are also observed [22].

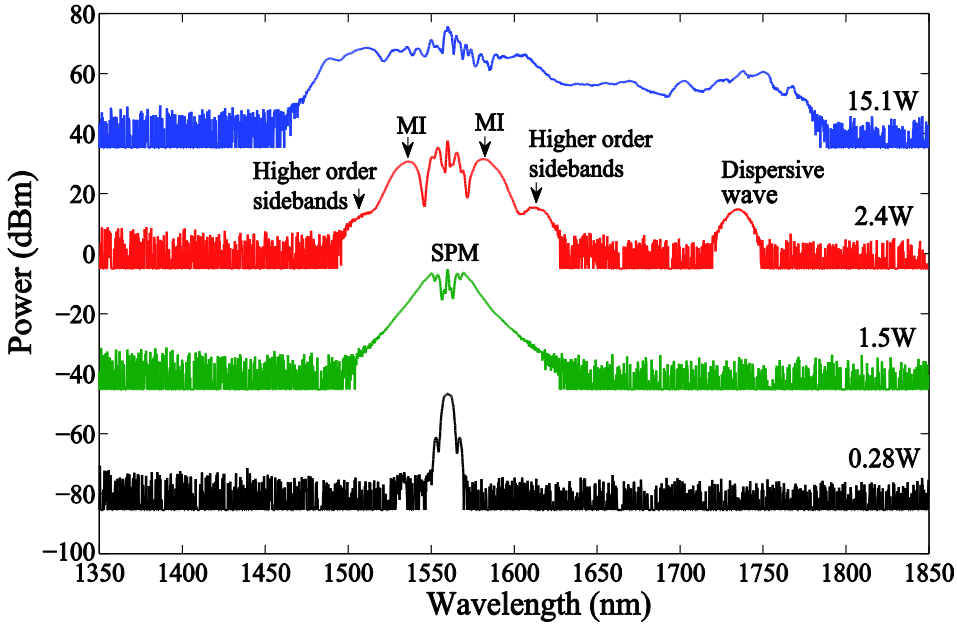

Fig. 1. SC generation in a 1cm long 500×220 nm^2 a-Si-H waveguide: output spectrum as function of on chip peak pump power. The spectra are vertically offset by multiples of 40 dB for clarity.

However, an unexpected peak is seen at 2.4 W peak pump power shifted by 19.4 THz from the pump. We discuss briefly the possible origin of this peak. The detuning of the peak changes approximately by 7 THz when changing the pump wavelength from 1560 nm to 1530 nm. This rules out a Raman shift, which would occur at fixed detuning. In addition, the Raman shift in amorphous silicon was measured to be around 14.5 THz [23]. The value of the dispersion (β_2=-2ps^2/m) of the waveguide has been estimated at telecommunication wavelengths from a four-wave-mixing based conversion efficiency spectrum at low power [18]. From this we deduce that the peak could not be generated by soliton fission, as the estimated nonlinear length and soliton fission length [2], of L_{NL}=476μm and L_{SF}=1.2cm (P=3W) respectively, do not allow for this process in a 1 cm long waveguide.

Having eliminated these two possibilities, the only known process that could produce this peak is Cherenkov radiation, also referred to as dispersive wave generation [24]. In particular it would result from the formation of pre-solitonic breathers along the pump pulse in a regime where modulation instability is the main nonlinear effect behind the supercontinuum generation, as reported in [25, 26]. To confirm this interpretation we would require a measurement of the dispersion of the waveguide. Unfortunately measurements of the dispersion are not available at present.

At the highest peak power, both parts are joined and the SC is flattened thanks to cascaded four wave mixing.

Concerning stability, we observed a decrease of SC bandwidth as a function of time due to optical degradation of the waveguide (Figure 2(a)). This process is faster during the first hour. It then reaches a kind of steady state regime where the degradation becomes very slow. Figure 2(b) depicts a comparison between SC spectra generated using a 1530 nm (FWHM≈1.6 ps, P_{peak}=6 W) pump wavelength at t=0 minutes and after 15 hours of illumination.

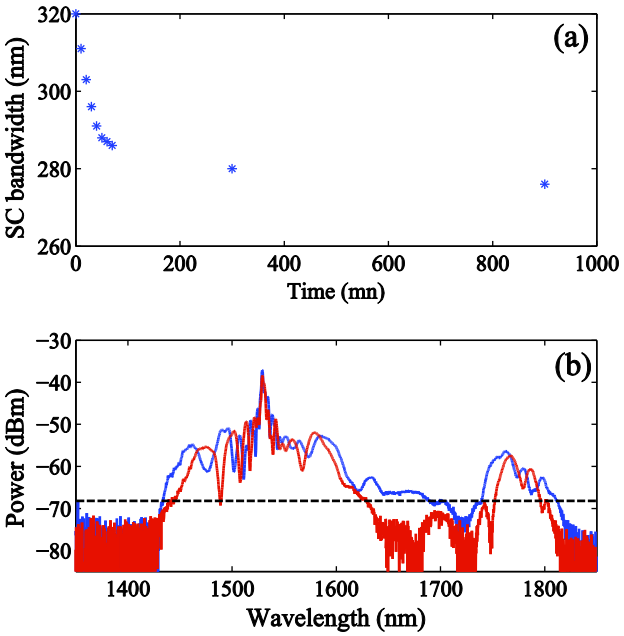

Fig. 2. (a) Evolution of the SC bandwidth as a function of time at -30 dBm from the pump peak. (b) Comparison between SC bandwidth at the beginning of the experiment (blue curve, t=0 minutes), and after degradation (red curve, t=15 hours). The dashed line represent the level at which the SC bandwidth evolution was calculated for panel (a).

This degradation probably originates from the Staebler-Wronski effect [27]. In 1975, Staebler and Wronski demonstrated that under illumination, thin-film amorphous silicon solar cells are not stable and their efficiency decreases over time [27]. A few years later, Stutzmann et al. found that this results from the degradation of the optical material properties, due to a process in which electron-hole pairs created by energetic photons recombine in the material [28]. In our case, high power pump pulses creates free carriers due to the presence of nonlinear absorption in a-Si-H waveguides. These free carriers can therefore degrade the material following the Staebler Wronski mechanism.
In a-Si-H waveguides the evolution of the degradation depends on pulse duration, it is much lower when shorter pulses are used. Annealing the sample at 200 °C for 5 minutes, allows to restore all the optical properties of the a-Si-H waveguides [21].

To study the role of the waveguide geometry on the SC bandwidth and stability, we performed other experiments in waveguides of 700 nm, 750 nm and 800 nm width and 1cm length (thickness 220 nm). In these experiments both waveguides facets are cleaved, and the lensed fiber to chip coupling losses at each facet are estimated to be close to10 dB. The output spectra for the three waveguides are depicted in figure 3. The best results are obtained for the 800nm wide waveguide for which a spectral broadening greater than 550 nm is observed with an on chip peak power as low as 4 W.

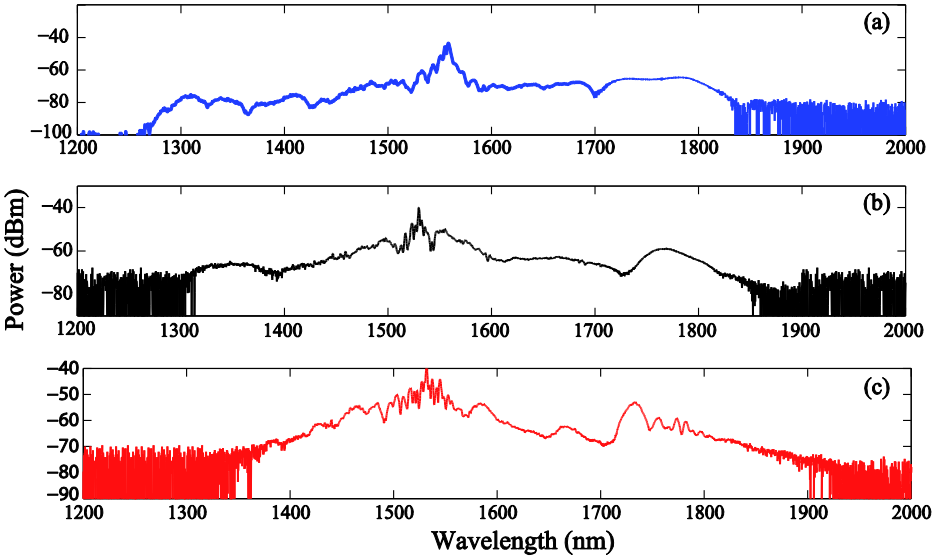

Fig. 3. SCs generation in 1 cm long a-Si-H waveguides with a cross-section of 700×220 nm^2 (a), 750×220 nm^2 (b), and 800×220 nm^2 (c) observed on a mid-IR OSA. In panel (a) the pump wavelength is 1560nm (FWHM ≈ 1 ps), while it is 1530 nm (FWHM ≈ 1.6 ps) in panel (b) and (c). The on chip peak power is 12 W, 9 W and 4 W respectively.

By following the spectrum evolution versus power, we observed that, similarly to the waveguide of 500nm width, SPM, MI and dispersive wave generation are the main processes responsible for the SC generation in all these waveguides.

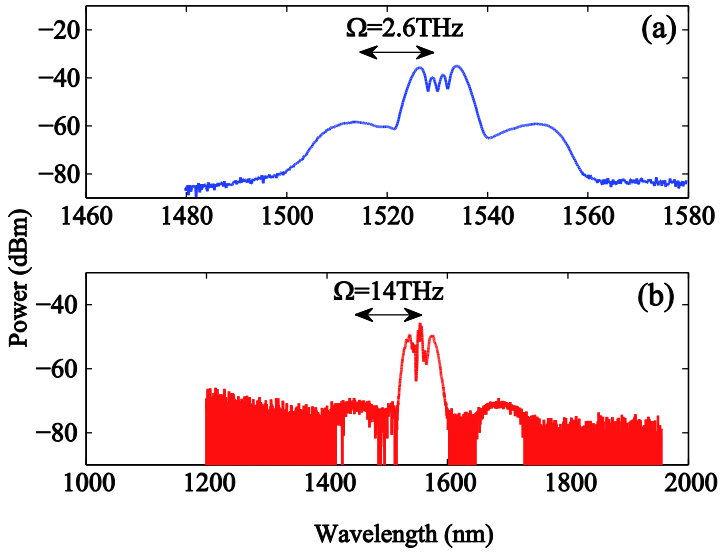

Fig. 4. Output spectra of MI process in 1cm long waveguides of cross section of 500×220 nm^2 (a) and 700×220 nm^2 (b) respectively. A 3.8 ps pulsed laser (power on chip =8 W) was used for the waveguide of 500 nm of width, and a 1.6 ps pulsed laser (power on chip = 3.3 W) for the waveguide of 700 nm of width.

Changing the waveguide width affects dispersion, which affects the nonlinear processes that give rise to the SC. This explains why the spectra observed in fig. 3 differ. In particular it is interesting to compare the detuning Ω of the modulation instability sideband between the waveguides of 500 nm and 700 nm width, see Fig. 4 (a) and (b). Larger detuning, due to an anomalous dispersion β_2 near to zero, is observed in the 700 nm wide waveguide, as predicted by the relation $\Omega = \sqrt{2\gamma_{real} P / \beta_2}$ [29]. This combined with the location of the dispersive wave, explains the greater spectral width of the SC in the wider waveguides.

In Table 2 we report the estimated values of the nonlinear coefficient γ_{real} and the nonlinear FOM. The nonlinear coefficient γ_{real} was estimated by fitting the observed SPM spectra of each waveguide with numerical simulations.

Table 2. Nonlinear coefficient and FOM as a function of waveguides width

Waveguides Width (nm)	500	700	750	800
Nonlinear coefficient γ_{real} $W^{-1}m^{-1}$	740	576±70	546±50	450±80
FOM	2.1	2.4±0.6	2.2±0.2	1.98±0.1

We were surprised to observe good stability of the SC over time in the wider waveguides, see figure 5 where the bandwidth is shown not to have changed after 1 hour of illumination in a 750 nm wide waveguide.
The same stability was observed in the 700 nm and 800 nm wide waveguides. In work that will be reported in detail elsewhere, we observed also high SC stability in waveguides of width 700 nm, 750 nm and 800 nm when femto-second pulses were used at telecommunication wavelength.

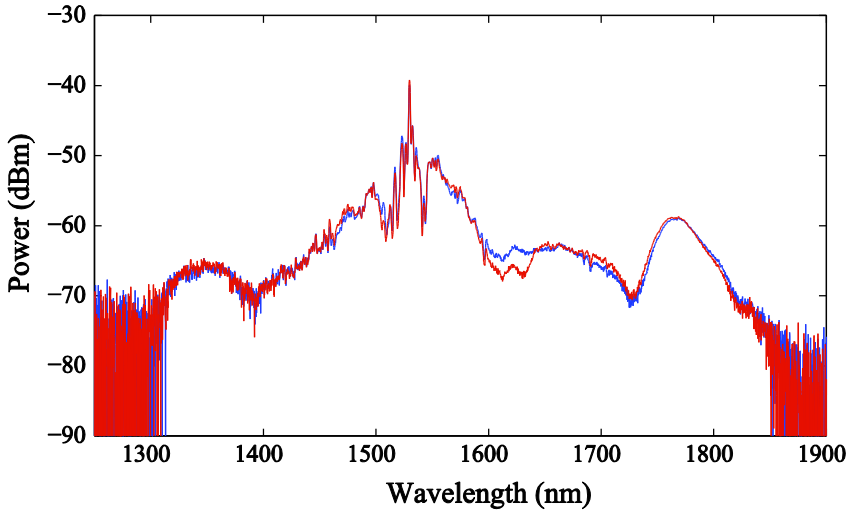

Fig. 5. Stability of the SC generated in a waveguide of 750 nm of width (blue curve (t=0 minutes), red curve (t=60 minutes)): after 1 hour the spectrum has not changed (compare with figure 3(b)).

This stability can originate from the lower degradation in the broad waveguides that can be partially attributed to the lower TPA, short pulse width and lower light intensity. However this

observation also indicates that the optical degradation is a highly nonlinear phenomenon, since small changes of the propagation conditions completely change whether or not degradation occurs. This could be due to the number or energy of the free carriers required for the Staebler-Wronski effect. We expect to report a more detailed study of optical degradation in a forthcoming paper.

3. Conclusion

We have demonstrated SC generation in 1 cm long CMOS compatible hydrogenated amorphous silicon waveguides. Using wide waveguides (up to 800 nm width) that provide very low dispersion, we demonstrated a spectral broadening greater than 550 nm around telecommunication wavelengths with a low on chip peak power of 4 W. Quite unexpectedly, we did not observe any optical degradation in the wider waveguides. These results highlight the potential of a-Si-H for integrated, on chip, non linear optics.

Acknowledgments.

The authors thank Stéphane Coen, Thibaut Sylvestre and Mathieu Chauvet for fruitful discussions. We acknowledge financial support by the FRS-FNRS and by the Inter-University Attraction Pole (IAP) project Photonics@be. Part of this work was carried out in the framework of the FP7-ERC projects MIRACLE and InSpectra.